THE JOURNAL OF BIOLOGICAL CHEMISTRY VOL. 290, NO. 15, pp. 9555–9570, April 10, 2015

Extracellular Processing of the Cartilage Proteoglycan Aggregate and Its Effect on CD44-mediated Internalization of Hyaluronan*

Received for publication, February 3, 2015, and in revised form, February 24 2015 Published, JBC Papers in Press, March 2, 2015, DOI 10.1074/jbc.M115.643171

Ben T. Danielson, Cheryl B. Knudson, and Warren Knudson[1]

From the Department of Anatomy and Cell Biology, Brody School of Medicine, East Carolina University, Greenville, North Carolina 27834

Background: The extracellular events that precede the endocytosis and turnover of hyaluronan are poorly understood.
Results: Progressive degradation of aggrecan results in a threshold size that permits hyaluronan endocytosis.
Conclusion: Hyaluronan internalization is controlled by changes in size of the macromolecule and its bound constituents.
Significance: The initial event in the turnover of hyaluronan is the extracellular cleavage of aggrecan.

In many cells hyaluronan receptor CD44 mediates the endocytosis of hyaluronan and its delivery to endosomes/lysosomes. The regulation of this process remains largely unknown. In most extracellular matrices hyaluronan is not present as a free polysaccharide but often is found in complex with other small proteins and macromolecules such as proteoglycans. This is especially true in cartilage, where hyaluronan assembles into an aggregate structure with the large proteoglycan termed aggrecan. In this study when purified aggrecan was added to FITC-conjugated hyaluronan, no internalization of hyaluronan was detected. This suggested that the overall size of the aggregate prevented hyaluronan endocytosis and furthermore that proteolysis of the aggrecan was a required prerequisite for local, cell-based turnover of hyaluronan. To test this hypothesis, limited C-terminal digestion of aggrecan was performed to determine whether a size range of aggrecan exists that permits hyaluronan endocytosis. Our data demonstrate that only limited degradation of the aggrecan monomer was required to allow for hyaluronan internalization. When hyaluronan was combined with partially degraded, dansyl chloride-labeled aggrecan, blue fluorescent aggrecan was also visualized within intracellular vesicles. It was also determined that sonicated hyaluronan of smaller molecular size was internalized more readily than high molecular mass hyaluronan. However, the addition of intact aggrecan to hyaluronan chains sonicated for 5 and 10 s reblocked their endocytosis, whereas aggregates containing 15-s sonicated hyaluronan were internalized. These data suggest that hyaluronan endocytosis is regulated in large part by the extracellular proteolytic processing of hyaluronan-bound proteoglycan.

The glycosaminoglycan hyaluronan (HA)[2] is a ubiquitous matrix macromolecule present in nearly all vertebrate tissues. HA turnover within most tissues occurs via two mechanisms, namely, local degradation within the tissue of origin and/or release of HA into the lymphatic and vascular systems (1–3) where it is taken up by receptors lining the endothelium and degraded. We (4–9) and others (10–13) have demonstrated that endocytosis via the HA receptor CD44 is a major mechanism used for local turnover of HA, one that results in the delivery of HA to lysosomes for complete breakdown. Local turnover of HA is of particular necessity in non-vascularized articular cartilage (14). For example, in studies on the turnover of newly synthesized HA in bovine cartilage explants, the release of HA into the medium represented only 9% of the total radiolabeled HA that was lost from the tissue (15).

In cartilage, HA participates in the retention of the proteoglycan aggrecan. Within the extracellular space, aggrecan is organized as a multicomponent aggregate composed of aggrecan monomers bound to a core filament of HA and stabilized by the association of link proteins (16). The HA-aggrecan-link protein complex is retained at the chondrocyte cell surface either via HA that maintains connections with an HA synthase or via HA bound to CD44 (17, 18). All three of these components of the aggrecan aggregate constantly undergo turnover in the pericellular and territorial matrix of healthy and osteoarthritic cartilage. For example, one of the early events associated with osteoarthritis is the pronounced loss of aggrecan from the cartilage (16). Aggrecan turnover occurs extracellularly because of cleavage of the core protein by endoproteinases termed aggrecanases as well as matrix metalloproteinases) (19–21). The aggrecanases ADAMTS-4 (22, 23) and ADAMTS-5 (20, 24–26) are thought to be the key mediators of aggrecan loss. C-terminal, chondroitin sulfate-rich fragments of aggrecan are lost from the cartilage by release into the synovial fluid (27, 28). In addition to aggrecan, a significant loss of HA is also observed in human osteoarthritic cartilage (29). A marked depletion of HA was observed in the articular cartilage

* This work was supported, in whole or in part, by National Institutes of Health Grants R01-AR43384 (to W. K.), R21 AR066581-01 (to W. K.), and R01-AR39507 (to C. B. K.).

[1] To whom correspondence should be addressed: Dept. of Anatomy and Cell Biology, Brody School of Medicine, East Carolina University, 600 Moye Blvd., Mailstop 620, Greenville, NC 27834-4354. Tel.: 252-744-2852; Fax 252-744-2850; E-mail: knudsonw@ecu.edu.

[2] The abbreviations used are: HA, hyaluronan; CP, clostripain protease; DMMB, dimethylmethylene blue; PG, proteoglycan; RCS, rat chondrosarcoma; TRU, turbidity-reducing unit.

of dogs following anterior cruciate ligament transection (30) or following reduced loading splint immobilization (31). In our previous studies, cultured explants of human articular cartilage treated with IL-1α displayed a loss of HA within the superficial and upper middle layers of cartilage, the same layers in which aggrecan loss also occurred (32). We have demonstrated that the other residual components of the aggrecan aggregate, namely the HA, together with bound aggrecan G1 domains and presumably link protein, are internalized by chondrocytes via a CD44-mediated mechanism (4, 7–9). The endocytosis of HA and aggrecan G1 domains (G1-ITEGE and G1-DIPEN) could be blocked by pretreatment of chondrocytes with anti-CD44-blocking antibodies (8), CD44 siRNA, or a CD44 dominant-negative construct (9). Additionally, no internalization of HA and G1-ITEGE was observed in murine *Cd44*$^{-/-}$ chondrocyte or fibroblast cultures (9).

Less is known of whether the turnover of aggrecan (an extracellular proteolytic processing event) and the turnover of HA (internalization and intracellular degradation) are in any way coordinated. Previous studies using radiolabeling of bovine articular cartilage explant cultures demonstrated that newly synthesized HA and proteoglycan (aggrecan) had nearly identical half-lives of ~13–25 days (15, 33). How these turnover rates could be similar giving the differing mechanisms involved remained to be clarified. We have shown previously, using bovine chondrocytes, that the addition of full-size aggrecan to HA limits the ability of HA to be internalized (8). This suggested a hypothesis that HA endocytosis occurs only after a sufficient degree of degradation of the large aggrecan monomers has occurred. In other words, there may be an overall size requirement for HA aggregates that inhibits or permits HA endocytosis. In the current study, HA endocytosis was examined in the presence and absence of bound aggrecan monomers of decreasing size. Partially degraded aggrecan species were obtained following limited, controlled C-terminal proteolysis of purified aggrecan monomers or digestion of HA/aggrecan aggregates. We demonstrate that the capacity for HA endocytosis by chondrocytes is dependent on changes in size of the aggrecan decorating the HA.

Rat chondrosarcoma (RCS) cells, an immortalized chondrocyte-like cell line, were used in this study. These cells exhibit similar maintenance of their HA and aggrecan cell-associated matrices as we observed previously on bovine and human articular chondrocytes (18). These cells display HA/aggrecan-dependent pericellular matrices that are retained at the cell surface via CD44 as well as the capacity for CD44-mediated endocytosis of HA (4, 18, 34). The retention of the HA/aggrecan pericellular matrix can be blocked with the use of anti-CD44 antibodies (18). Of importance to this kind of study, RCS cells maintain the chondrocyte phenotype when attached to glass chamber slides.

EXPERIMENTAL PROCEDURES

Materials—DMEM was obtained from Mediatech (Herndon, VA), and FBS was purchased from Hyclone (South Logan, UT). High molecular mass HA (1.2–1.8 MDa), mid-HA (180–350 kDa), and low molecular mass HA (<5 kDa) were from Lifecore Biomedical (Chaska, MN). Agarose and Tris acetate-EDTA buffers were from IBI Scientific (Peosto, IA), and the 1-kb DNA ladder was from Thermo Fisher Scientific (Waltham, MA). Stains-all reagent was from MP Biomedicals (Solon, OH). All other enzymes and chemicals either molecular biology or reagent-grade materials were purchased from Sigma-Aldrich.

Cell Culture—The RCS cell line is a continuous long-term culture line derived from the Swarm rat chondrosarcoma tumor (35). The RCS cell line in the Knudson laboratories was a gift from Dr. James H Kimura (formerly of Rush University Medical Center) and represents an early clone of cells that eventually became known as long-term culture RCS (36). RCS chondrocytes were cultured as high density monolayers (2.0×10^6 cells/cm^2) in DMEM containing 10% FBS and 1% L-glutamine and penicillin-streptomycin and incubated at 37 °C in a 5% CO_2 environment. The RCS cells were passaged at confluence using 0.25% trypsin/2.21 mM EDTA.

Isolation and Purification of Aggrecan from Bovine Articular Cartilage—Full thickness slices of bovine articular cartilage were excised from 18–24-month bovine metacarpophalengeal joints obtained from the local abattoir (37). The cartilage was frozen in liquid nitrogen, ground to a powder, and extracted in dissociative buffer consisting of 4.0 M guanidine HCl, 0.01 M EDTA, and 0.05 M sodium acetate, pH 5.8 (38, 39). After gentle stirring at 4 °C for 24 h, the solution was centrifuged at 13,000 × *g* and brought to a final density of 1.5 g/ml by the addition of 0.5452 g of CsCl/ml. Samples were centrifuged at 100,000 × *g* for 48 h at 4 °C in a Beckman 50.2Ti rotor. Upon completion, the bottom fifth of each centrifuge tube was isolated, dialyzed against water for 3 days, and lyophilized.

Clostripain Digestion of Aggrecan—Clostripain from *Clostridium histolyticum* was diluted to 5 units/ml (20 μg/ml) in 0.6 mM dithiothreitol/5.0 mM CaCl, and the enzyme was activated by incubating at 37 °C for 3 h (40, 41). Purified aggrecan (6.0 mg/ml) or HA/aggrecan aggregates (0.5–1.0 mg/ml) dissolved in 0.1 M Tris/0.1 M $NaC_2H_3O_2$ were mixed 1:1 (v/v) with the activated clostripain solution (40). At various times, the enzymatic activity was deactivated by the addition of iodoacetamide to a final concentration of 1.1 mM. Digested proteoglycan-containing preparations were then precipitated by adjustment of the solution to 70% (70 ml/100 ml) ethanol containing 1.3% (1.3 g/100 ml) potassium acetate followed by centrifugation at 1,300 × *g* for 10 min at 4 °C. The resulting pellet was allowed to dry thoroughly in a chemical hood.

Preparation of Fluorescent HA and Aggrecan—Fluorescein-conjugated hyaluronan (FITC-HA) was prepared as described previously (4, 7) using high molecular mass (1.2–1.8 MDa) research-grade HA as the substrate. After conjugation, the FITC-HA was precipitated by an adjustment to 70% ethanol containing 1.3% (w/v) potassium acetate. After centrifugation at 1,300 × *g* for 10 min at 4 °C, the resulting pellet was allowed to dry thoroughly in a dark chemical hood. The dried pellet was resuspended in culture media containing 10% FBS at a final concentration of 1 mg/ml. To prepare shorter length HA, a FITC-HA sample was cooled in an ice bath and sonicated with a microtip probe at output level 6 for 5–30 s using a W-220 sonicator ultrasonic processor (Heat Systems-Ultrasonic, Plainview, NY). The aggrecan monomer or aggregate was labeled with dansyl chloride using the method of Tenglad (42) and

Bartzatt (43). Briefly, 6 mg of purified aggrecan monomer or aggregate was dissolved in 1 ml of distilled water. The solution was then mixed with an equal volume of 2 M Na_2CO_3 (pH 11). Then 5 mg of dansyl chloride (Alfa Aesar, Heysham, England) in 1 ml of acetone was slowly added to the mixture with stirring, and the mixture was allowed to sit at room temperature for 1 h in the dark. The mixture was then ethanol precipitated in 70% ethanol containing 1.3% (w/v) potassium acetate and centrifugation at 1,300 × *g* for 10 min at 4 °C. The resulting pellet was allowed to thoroughly dry in a dark chemical hood and resuspended in media + 10% FBS or in 0.1 M Tris, 0.1 M $NaC_2H_3O_2$ buffer.

Agarose Gel Electrophoresis—HA and proteoglycans were separated on 1% agarose gels prepared in Tris acetate-EDTA buffer and cast into 10 × 15-cm trays of a MP-1015 horizontal electrophoresis apparatus (ISI Scientific) (44–46). Samples (15 μl) were loaded into each well with one well loaded with 5 μl of a 1 kb-PLUS DNA ladder (1,000–12,000 bp) for reference. Electrophoresis was carried out for 30 min at 150 V. Gels were first visualized by UV transillumination and fluor imaging detection using a ChemiDoc imager (Bio-Rad). Gels were then fixed by rinsing them in 70% ethanol for 30 min and stained overnight with Stains-all or dimethylmethylene blue (DMMB) followed by destaining in 70% ethanol. The stained bands were imaged by trans-white light on the ChemiDoc imager.

Particle Exclusion Assay—RCS chondrocytes were cultured overnight in 35-mm wells. The medium was replaced with a suspension of formalin-fixed erythrocytes in PBS/0.1% BSA (17). Cells were photographed using a Nikon TE2000 inverted phase-contrast microscope, and images were captured digitally in real time using a Retiga 2000R digital camera (QImaging, Surrey, British Columbia, Canada). The presence of cell-bound extracellular matrix is seen as the particle-excluded zone surrounding the chondrocytes.

Fluorescence Microscopy—For immunofluorescence studies, RCS cells were plated into 4-well chamber slides at 12,000 cells/well and cultured for 24 h. Prior to assay, the cell monolayers were treated for 20 min at 37 °C with 200 turbidity-reducing units (TRU)/ml of bovine testicular hyaluronidase or 5 units/ml *Streptomyces* hyaluronidase prepared in media containing 10% serum. The HA-free cells were then rinsed repeatedly and incubated with FITC-HA or FITC-HA/aggrecan aggregates at varying concentrations for 3 h at 4 °C to visualize total extracellular binding or for 24 h at 37 °C to visualize internalized HA. After incubation, cells were rinsed with PBS and fixed directly (to visualize total binding) or, post-treated with 5 units/ml *Streptomyces* hyaluronidase (to visualize internalized HA and aggrecan) prior to fixation in 4% paraformaldehyde for 10 min at room temperature. The fixed cells were quenched with 0.2 M glycine in PBS and mounted using medium containing DAPI nuclear stain. The accumulation of FITC-HA was visualized using a Nikon Eclipse E600 microscope equipped with Y-Fl Epi fluorescence, a 60 × 1.4 n.a. oil-immersion objective, and FITC (green) and DAPI (blue) filters. Images were captured digitally using a Retiga 2000R digital camera and processed using NIS-Elements BR, version 1.30, imaging software (Nikon, Lewisville, TX).

To prevent intracellular lysosomal degradation of FITC-HA, the RCS chondrocyte culture media contained 25 μM chloroquine during the endocytosis incubation period. Preliminary studies (not shown) determined that the standard 100 μM concentration of chloroquine often used by investigators (47, 48) was toxic for RCS cells. A chloroquine concentration of 25 μM was found sufficient to prevent acidification of lysosomes (eliminate LysoTracker Red staining for low pH organelles) but non-toxic for these cells.

Morphometric Analysis of Fluorescence Microscopy Images—Changes in the mean pixel intensity of FITC-HA bound to or localized within RCS chondrocytes were quantified using NIS-Elements BR2.30 imaging software (Nikon). Single region-of-interest squares of equal size (area = 55 μm^2) were placed over each cell within a field of view to be quantified. Three squares of similar size were placed over cell-free areas within the field for determination of background intensities. The mean, maximal, and summed intensities were determined for each region of interest represented on each of the 12-bit gray-scale cell images (0–4095 relative intensity values). Twenty-five to 30 cells were analyzed for each condition within a separate experiment. Values from multiple experiments were then normalized and used for statistical quantification of results.

Statistical Analysis—All data were obtained from at least three independent experiments performed in duplicate or triplicate. Statistical significance was determined using the two-tailed unpaired Student's *t* test. A *p* value of less than 0.05 was considered significant.

RESULTS

Analysis of Purified Aggrecan Monomers—Aggrecan monomer was isolated from young bovine metacarpophalangeal joint cartilage following extraction of pulverized tissue with 4 M guanidine HCl. The cartilage extract was centrifuged in a CsCl gradient under dissociative conditions to yield a D1 fraction containing proteoglycan monomer. The physical properties of this aggrecan preparation were analyzed by electrophoresis on 1% agarose gels. Agarose gel electrophoresis has been used in recent years (44–46, 49, 50) to separate various sizes of HA as shown in Fig. 1*A*. Reasonable separations can be achieved of high, middle, and low molecular mass HA as well as FITC-conjugated HA species detectable by UV transillumination (Fig. 1*B*). Under these same conditions, the D1 fraction-aggrecan monomers ran as a unimodal but disperse band midway between high and middle molecular mass HA standards (Fig. 1, *C* and *D*). No change in the migration of the aggrecan monomer was observed following treatment with *Streptomyces* hyaluronidase, suggesting little contamination by HA present in the neighboring D2 fraction of the CsCl gradient. As a positive control, high molecular mass HA treated with *Streptomyces* hyaluronidase migrated to a region of small oligosaccharides within the gel (Fig. 1*C*, *lane 2*). The aggrecan monomer exposed to exhaustive treatment with clostripain protease (CP) shifted to faster migrating bands, indicative of degradation of the proteoglycan core protein (Fig. 1, *C*, *lane 5*, and *D*, *lane 4*). In Fig. 1*D*, the *panel* was stained with DMMB, indicative of sulfated glycosaminoglycans such as keratan sulfate and chondroitin sulfate; HA (in *lane 1*) was not detected by DMMB.

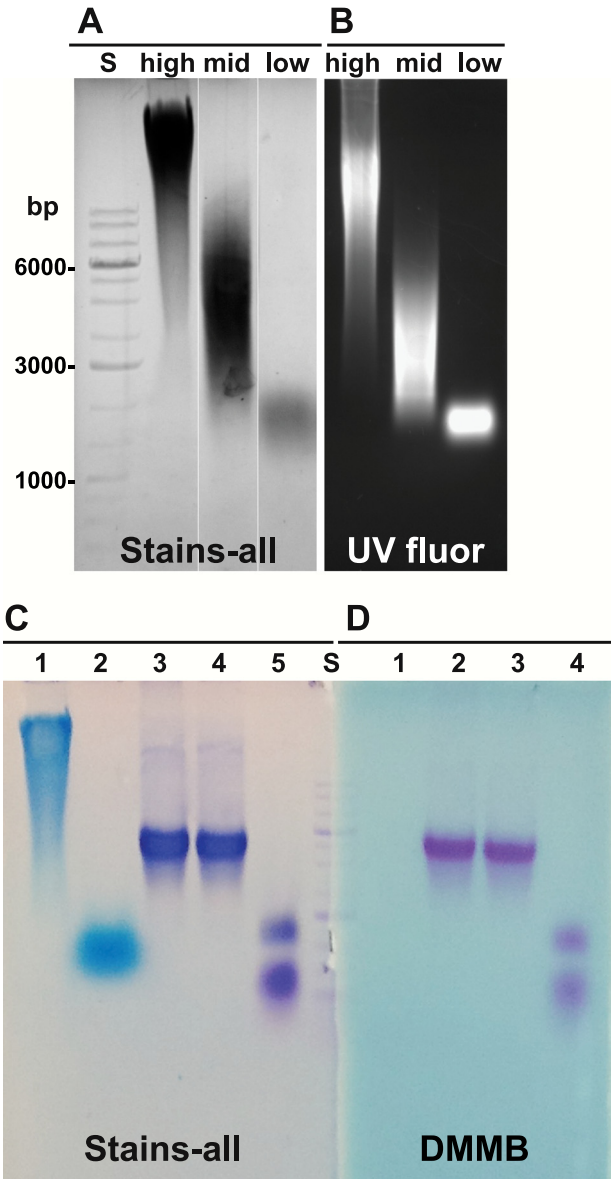

FIGURE 1. **Analysis of purified aggrecan monomers.** Three commercially available HA standards were analyzed by electrophoresis on 1% agarose gels at a concentration of 1 mg/ml and detected with Stains-all reagent (*A*, shown in gray scale). *High*, HA of 1,200–1,800 kDa; *mid*, HA of 180–350 kDa; *low*, HA < 5 kDa. The same HA samples were conjugated with FITC, and following electrophoresis visualized with transillumination UV fluorescence (*B*, *UV fluor*). Aggrecan was purified from cartilage slices derived from bovine metacarpophalangeal joints. Aliquots of the purified aggrecan D1 fraction (*C*, *lanes 3–5*, and *D*, *lanes 2–4*) and high molecular mass HA (*C* and *D*, *lane 1*) were electrophoresed on 1% agarose gels and detected using Stains-all (*C*) or DMMB (*D*). Some samples were predigested with *Streptomyces* hyaluronidase (*C*, *lanes 2* and *4*, and *D*, *lane 3*) or clostripain protease (*C*, *lane 5*, and *D*, *lane 4*) prior to electrophoresis. A 1-kb DNA ladder standard (*S*) was used for reference and alignment of the gel; critical bands are labeled in *A*. The data shown in *C* and *D* are a representative example of four replicated, independent experiments.

Visualization of HA and Reconstituted Aggregate—To verify that the purified aggrecan monomer retained a functional capacity to bind to HA, the D1 aggrecan monomer was mixed in varying proportions with a fixed concentration of FITC-HA and allowed to re-aggregate. Fig. 2*A* depicts Stains-all detection of FITC-HA and aggrecan monomers. Upon re-aggregation, HA/aggrecan aggregates exhibited a size shift wherein most of the aggrecan visualized by DMMB staining (Fig. 2*B*) was now detected in the loading wells of the agarose gel. The same gel under UV transillumination, which detects FITC-HA exclusively, showed a size shift of the HA that co-localized with aggrecan in the loading wells (Fig. 2*C*). It is important to note that a minimal ratio of aggrecan to FITC-HA of ~2:1 was required to consistently obtain a complete size shift of the FITC-HA (Fig. 2*C*). It should also be noted that a small percentage of the aggrecan monomer population does not exhibit a size shift in the presence of HA (Fig. 2*B*).

Another approach to verify the functionality of the D1 aggrecan fraction was to observe its ability to bind to endogenous HA on live cells in culture. A particle exclusion assay was used to visualize the presence of pericellular matrices surrounding our model chondrocyte cell line, the RCS cells. Fig. 2*D* depicts the small particle-excluding coats present on RCS cells after 48 h of culture in monolayer. As we have shown previously (17, 18, 34), these pericellular matrices are dependent on HA as a scaffold, as pretreatment of the RCS cells with 5 units/ml *Streptomyces* hyaluronidase removed the coat, allowing the particles to abut the plasma membrane (Fig. 2*F*). When fresh medium containing 2 mg/ml aggrecan monomer was added to the RCS cells for 1 h, large particle-excluding coats, up to 1-cell-diameter in size, were now observed (Fig. 2*E*). Post-treatment of cells (as in Fig. 2*E*) with *Streptomyces* hyaluronidase resulted in a rapid depletion of the pericellular matrix (Fig. 2*G*). These experiments demonstrate that the purified D1 aggrecan monomer is functionally competent to reconstitute with HA into an aggregate structure and contains sufficient glycosaminoglycan substitution to support assembly of a robust, hydrated, pericellular matrix typically associated with primary chondrocytes.

Total HA and HA/Aggrecan Aggregate Binding to Cells—The goal of this study was to determine the extent to which the binding of aggrecan to HA filaments affects HA endocytosis. As such, it was first necessary to demonstrate that FITC-HA, with or without bound aggrecan monomers, bound in an equivalent fashion to the plasma membrane/pericellular matrix of the RCS cells. Hyaluronidase-pretreated cultures were incubated with medium containing FITC-HA alone or FITC-HA/aggrecan aggregates for either 3 h at 4 °C (Fig. 3, *A*, *C*, and *E*) or 24 h at 37 °C (Fig. 3, *B*, *D*, and *F*). Hereafter, aggrecan will be designated simply as proteoglycan (PG), FITC-HA as HA, and FITC-HA/aggrecan aggregates as HA + PG. Nearly equivalent fluorescence was observed between RCS cultures incubated with HA alone (Fig. 3, *C* and *D*) or with HA + PG (Fig. 3, *E* and *F*). Cultures held at 4 °C presumably depict HA or HA + PG retained exclusively at the cell surface with little internalization (Fig. 3, *C* and *E*). Cultures incubated for 24 h at 37 °C represent intracellularly and extracellularly localized FITC-HA (Fig. 3, *D* and *F*). However, the majority of the punctate, clustered fluorescence observed in Fig. 3, *D* and *F*, is extracellular and sensitive to trypsin or *Streptomyces* hyaluronidase, as shown in Fig. 4. The mean pixel intensity of cells illustrated in Fig. 3 was quantified with the subtraction of background (Fig. 3, *A* and *B*) and included cells from other fields of view. Box plots of the representative experiments, shown at both 4 °C (Fig. 3*G*) and 37 °C (Fig. 3*H*), demonstrate nearly equivalent binding of FITC-HA (−) and HA + PG (+). The *bar graph* of percent

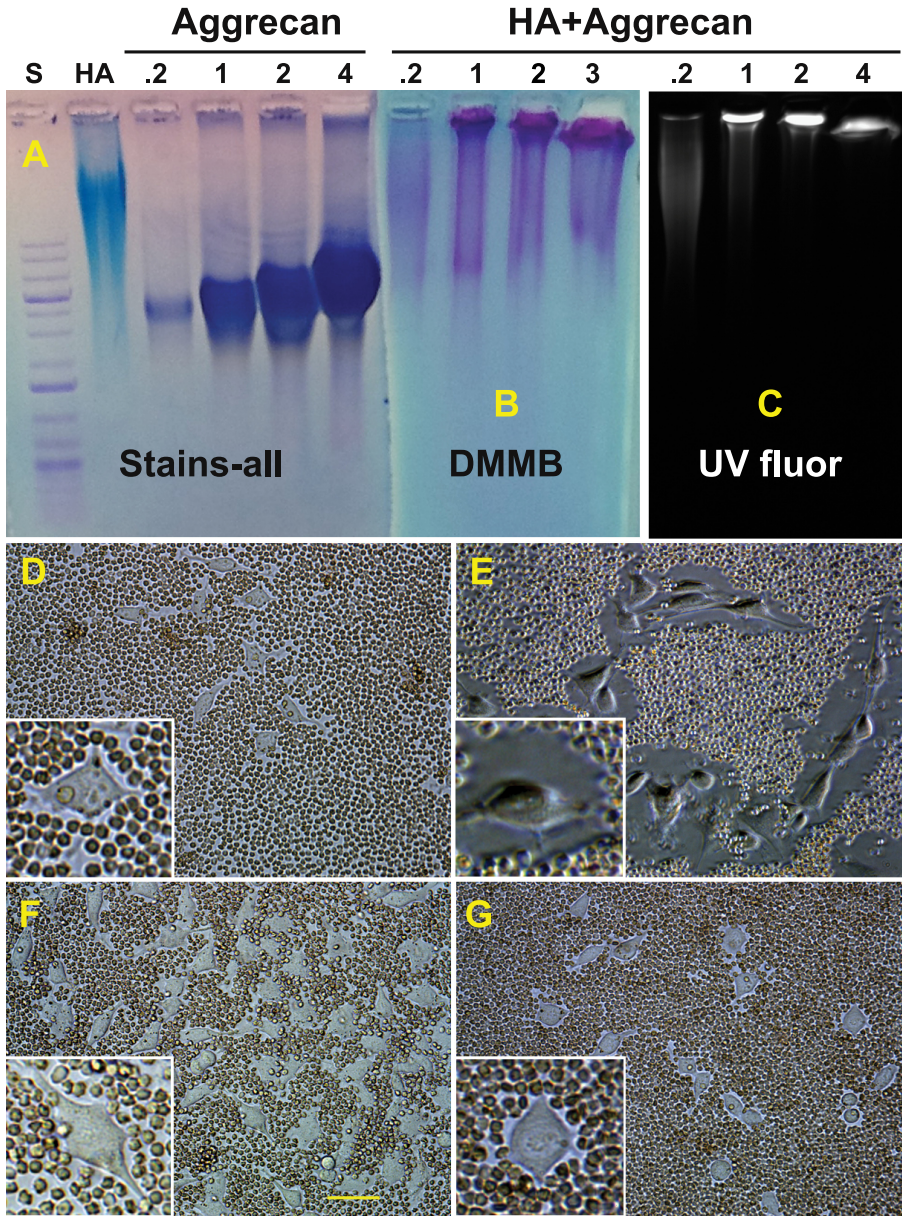

FIGURE 2. **Visualization of HA and reconstituted aggregates.** The ability of the purified aggrecan (D1 fraction) to form stable aggregates with HA was analyzed by observing size changes on 1% agarose gels following electrophoresis under non-dissociative conditions. Undecorated FITC-HA (*HA*) and various concentrations of aggrecan monomer (0.2–4.0 mg/ml) were first visualized with Stains-all (*A*). Reconstituted aggregates were then established using a fixed concentration (500 μg/ml) of high molecular mass FITC-HA, combined with varying concentrations of aggrecan monomers (0.2–4.0 mg/ml) prior to electrophoresis on 1% agarose gels. Band locations were then visualized by DMMB staining (*B*) or by transilluminator UV fluorescence (*C*). Next, a particle exclusion assay was used to visualize the pericellular matrix that surrounds live cells. *D*, control RCS cells with no treatment. *E*, RCS cells after the addition of 2.0 mg/ml aggrecan. *F*, RCS cells pretreated with *Streptomyces* hyaluronidase prior to the addition of aggrecan. *G*, RCS cells as in *E*, post-treated with *Streptomyces* hyaluronidase. High power images of individual cells are shown as *insets* (*D–G*). The data shown in *D–G* are a representative example of five replicated, independent experiments. The *bar* in *F* is 20 μm and is also applicable to *D–G*.

change of averaged mean pixel intensities of the HA + PG conditions, as compared with HA alone (value set to 100%), from four independent experiments performed at 4 °C (Fig. 3*I*) again demonstrates that the differences between total binding of HA (−) and HA in the presence of PG (+) were not significant.

Effect of Aggrecan on HA Endocytosis by RCS Cells—To more reliably visualize the internalized pool of FITC-HA, RCS cells were post-treated with either *Streptomyces* hyaluronidase or trypsin after incubations with HA or HA + PG for 24 h at 37 °C. Both of these conditions removed extracellularly exposed HA and HA + PG. As shown in Fig. 4, *C* and *D*, FITC-HA added alone was observed primarily within intracellular, perinuclear organelles as we had shown previously in rat, bovine, and human chondrocytes as well as pCD44-transfected COS-7 cells (4, 6–8). It should also be noted that the RCS cells were treated with an optimal concentration of chloroquine to block lysosomal degradation. Thus, the fluorescence observed in Fig. 4 (and Figs. 6–8) represents accumulated ligand internalized over the incubation period. When RCS cells were incubated with HA + PG, *green* fluorescent vesicles were observed, but the fluorescence intensity was substantially reduced (Fig. 4, *E* and *F*). The difference between endocytosis of HA alone (−)

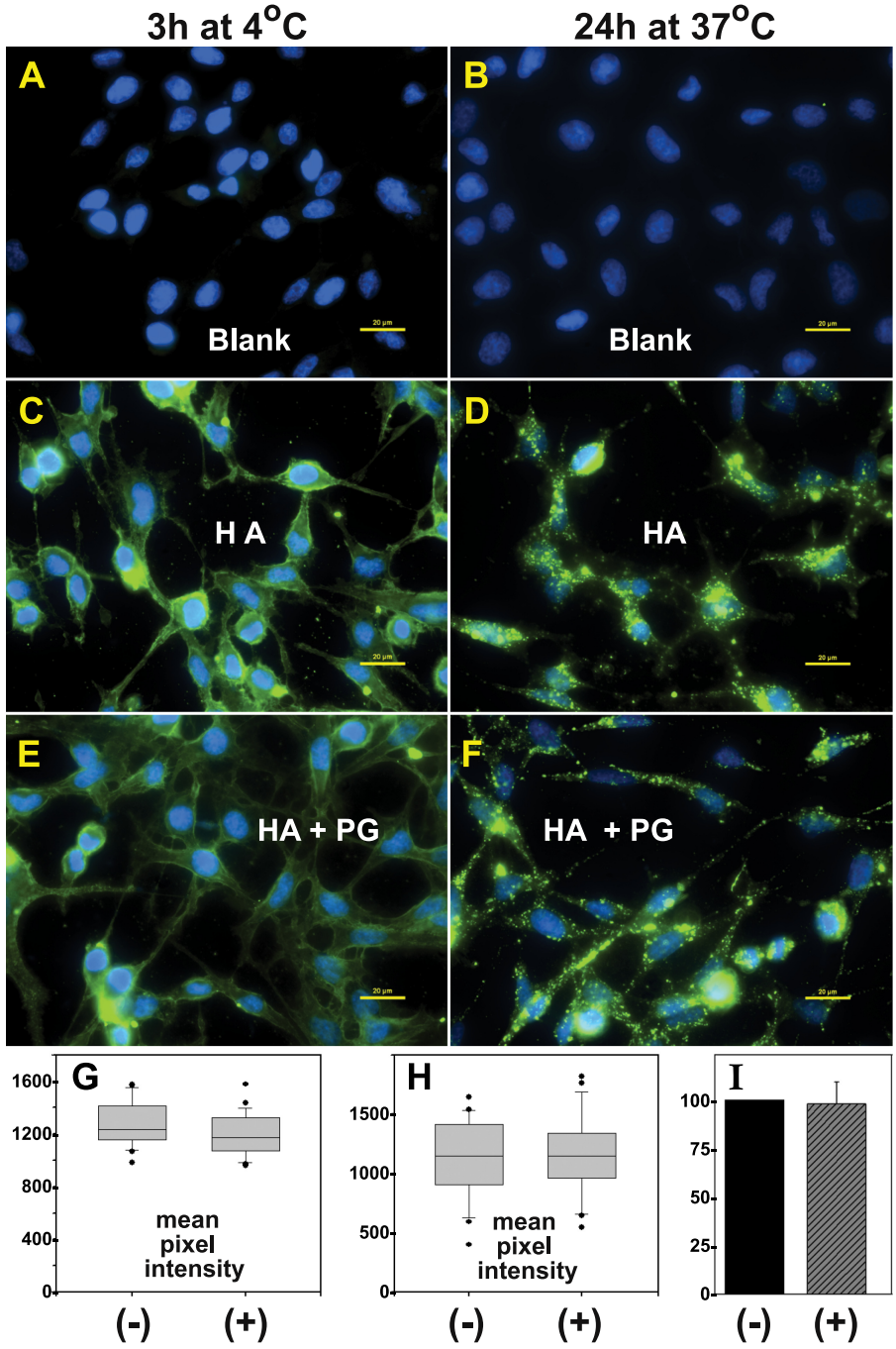

FIGURE 3. **Binding of total HA and HA/aggrecan aggregates to cells.** RCS cells grown in chamber slides were treated with 200 TRU/ml bovine testicular hyaluronidase, washed extensively, and then incubated for 3 h at 4 °C (*A*, *C*, and *E*) or 24 h at 37 °C (*B*, *D*, and *F*) in control medium (*A* and *B*, *Blank*), medium containing FITC-HA alone (*C* and *D*, *HA*), or aggregates of FITC-HA + aggrecan (*E* and *F*, *HA + PG*). The washed cells were then fixed, mounted in medium containing DAPI nuclear stain, and visualized by fluorescence microscopy. Shown are representative digital overlay images of *green* (HA) and *blue* (nucleus) fluorescence channels. The images shown are representative experiments from six independent experiments performed at 4 °C and three independent experiments performed at 37 °C. All *bars* are 20 μm. The mean pixel intensity of 25–30 cells/each experimental condition was evaluated for experiments performed at 4 °C (*G*) and 37 °C (*H*). Shown are the box plots of mean pixel intensities in RCS cells treated with FITC-HA without (−) or with (+) the inclusion of purified aggrecan. The mean pixel intensities of cells recorded as outliers are included and shown as *round dots* (●). The *bar graph* in *I* represents the mean pixel intensity average ± S.D. of six independent experiments performed at 4 °C and is illustrated as the normalized percent change in mean pixel intensity of HA + PG-treated cells (+), as compared with RCS cells treated with HA alone (−), set to 100%.

and HA + PG (+) was verified by quantification of mean pixel intensities following post-treatment with *Streptomyces* hyaluronidase (Fig. 4, *G* and *I*) and trypsin (Fig. 4*H*). Trypsin post-treatment generated more uniform rounded cells but ones that were released into suspension and more difficult to image in a single plane of focus. Cells remained attached to the substratum following post-treatment with *Streptomyces* hyaluronidase, and this condition was used for all subsequent experiments.

Limited C-terminal Cleavage of Aggrecan with Clostripain Protease—Purified aggrecan was incubated with clostripain protease under conditions optimized to affect a limited digestion of the proteoglycan within a workable time period. First,

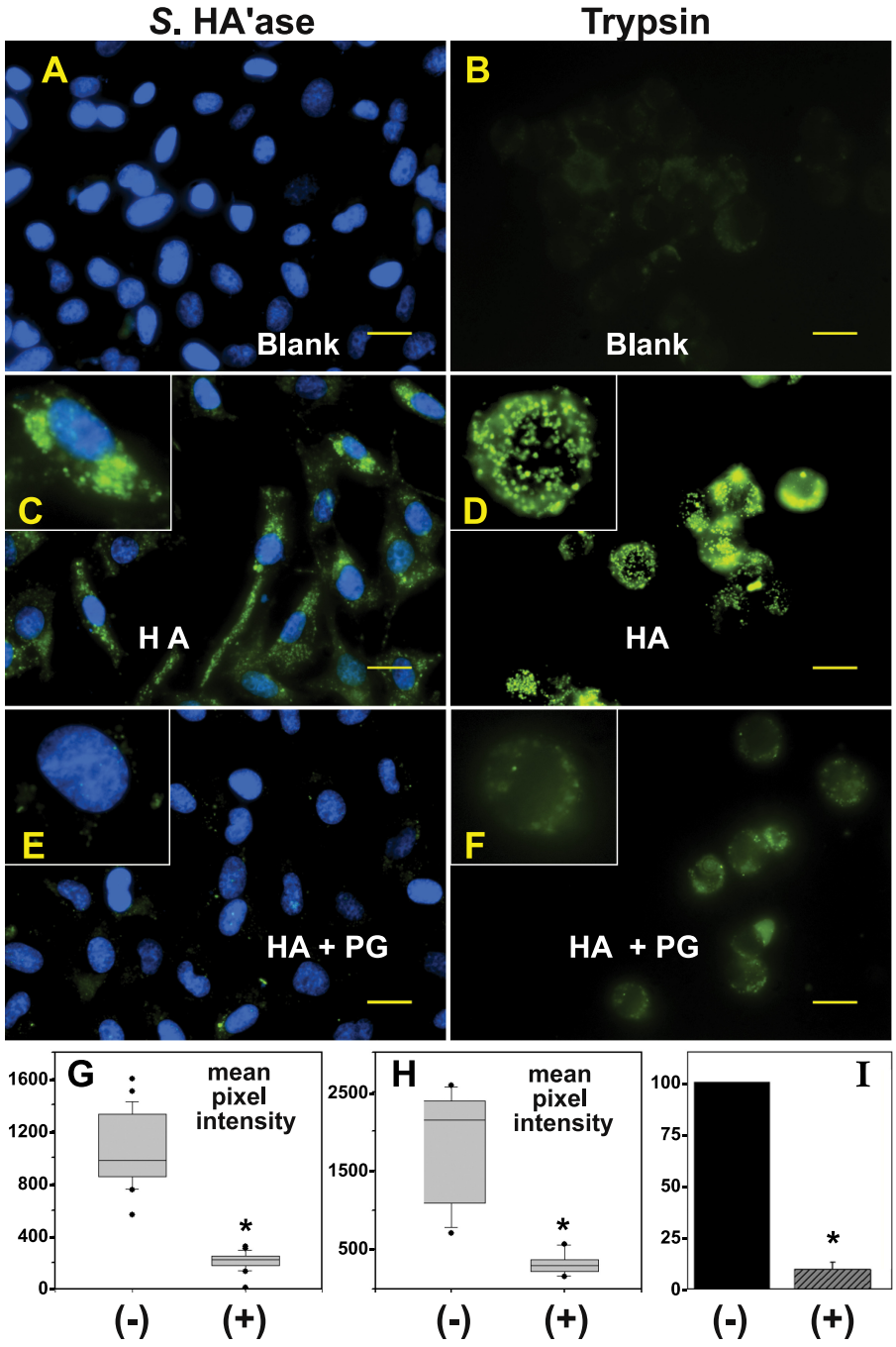

FIGURE 4. **Effect of aggrecan on HA endocytosis.** RCS cells grown in chamber slides were treated with 200 TRU/ml bovine testicular hyaluronidase, washed extensively, and then incubated for 24 h at 37 °C in control medium (*A* and *B*, *Blank*), medium containing FITC-HA alone (*C* and *D*, HA), or FITC-HA + aggrecan aggregates (*E* and *F*, *HA + PG*). The washed cells were then treated with *Streptomyces* hyaluronidase (*A*, *C*, and *E*, *Streptomyces* hyaluronidase) or trypsin (*B*, *D*, and *F*) to remove all extracellularly localized glycosaminoglycan. The *Streptomyces* hyaluronidase-treated cells were additionally fixed and mounted in medium containing DAPI nuclear stain. Both *Streptomyces* hyaluronidase- and trypsin-treated cells were visualized by fluorescence microscopy. Shown are digital overlay images of *green* (HA) and *blue* (nucleus) fluorescence channels. The images shown are representative experiments from eight independent experiments with *Streptomyces* hyaluronidase post-treatment and three independent experiments performed with trypsin post-treatment. All *bars* are 20 μm. The mean pixel intensity of 25–30 cells/each experimental condition was evaluated for experiments with post-treatment by *Streptomyces* hyaluronidase (*G*) or trypsin (*H*). Shown are the box plots of the mean pixel intensities in RCS cells treated with FITC-HA without (−) or with (+) the inclusion of purified aggrecan. The mean pixel intensities of cells recorded as outliers are included and shown as *round dots* (●). The *bar graph* in *I* represents the mean pixel intensity average ± S.D. of eight independent experiments with *Streptomyces* hyaluronidase post-treatment and illustrates the normalized percent change in mean pixel intensity of HA + PG-treated cells (+) as compared with RCS cells treated with HA alone (−) set to 100%. The *asterisks* denote $p < 0.05$.

aggrecan was incubated with clostripain as a free monomer (Fig. 5*A*). A modest shift in migration on agarose gels was observed for aggrecan monomers exposed to clostripain with increasing incubation time at 37 °C (Fig. 5*A*). When these fractions were ethanol-precipitated and redissolved in the presence of HA to allow for re-aggregation, fractions at all time points still exhibited a shift in migration into the loading wells (Fig. 5*B*). An increase in non-shifted, DMMB-positive proteoglycan was also observed. Next, when aggrecan was exposed to clostripain as an HA + PG aggregate (Fig. 5*C*), DMMB-positive pro-

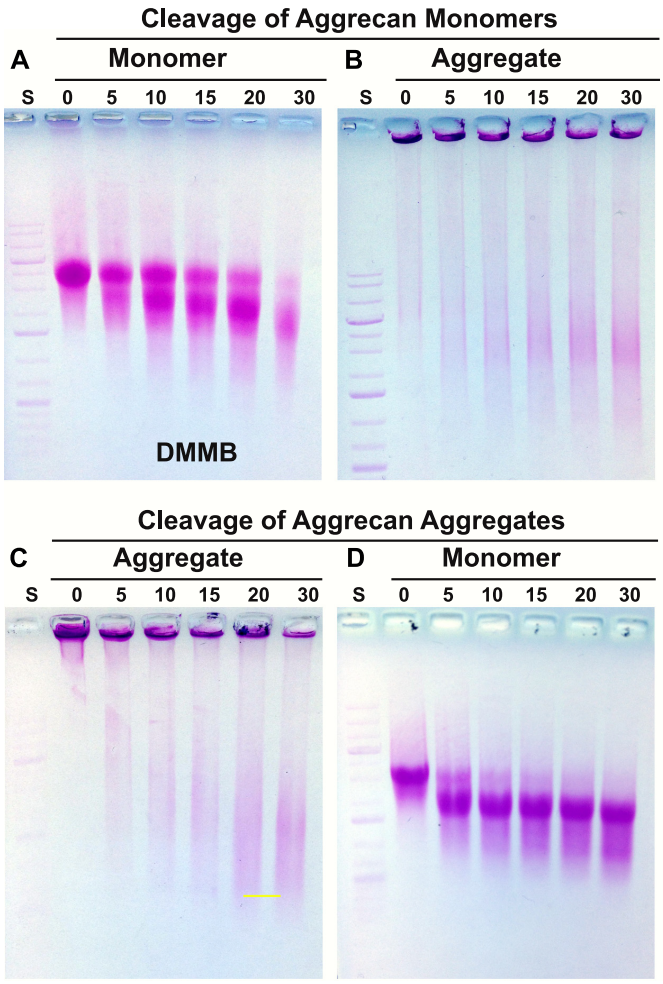

FIGURE 5. **Limited C-terminal cleavage of aggrecan with clostripain protease.** Aggrecan, either as a free monomer (*A* and *B*) or in an aggregate bound to HA (*C* and *D*), was digested for 0–30 min with clostripain protease and then evaluated directly by electrophoresis on 1% agarose gels stained with DMMB. Individual clostripain-digested monomer fractions (as in *A*) were next incubated with HA to reconstitute aggregates and re-evaluated on agarose gels (*B*). Individual clostripain-digested aggregate fractions (as in *C*) were subsequently treated with *Streptomyces* hyaluronidase to degrade the HA and return the aggrecan to monomers, and they were re-evaluated on agarose gels (*D*). Shown are representative images from four experiments. A 1-kb DNA ladder standard (*S*) was used for reference and alignment of the gel.

teoglycan remained in the loading wells of each time point. As in the digestion of monomers (Fig. 5*B*), a time-dependent increase of faster migrating proteoglycan was also observed. At each time point the clostripain-digested HA+PG fractions were subsequently post-treated with *Streptomyces* hyaluronidase to release the PG within aggregates back to PG monomers. As with the clostripain-digested monomers (Fig. 5*A*), a modest shift in proteoglycan monomer size was observed (Fig. 5*D*). These results suggest that the clostripain conditions used provided for limited cleavage of aggrecan. Given that similar results were obtained when using monomer or aggregate as substrate, N-terminal protection of aggrecan (protection afforded by digestion of the HA + PG aggregate) was not a major necessity. The results observed are consistent with clostripain cleavage that was predominately C-terminal. Because the aggrecan monomer was more readily dissolved following post-clostripain ethanol precipitation/purification, the remaining experiments utilized clostripain-treated monomers.

Effect of Limited C-terminal Cleavage of Aggrecan on HA Endocytosis—Aggrecan monomers were treated with clostripain protease for 0–60 min, precipitated and then reconstituted with FITC-HA into HA + PG. The migration of FITC-HA on agarose gels shifted into the loading wells when recombined with the 0- and 10-min treated monomers but displayed little movement when incubated with aggrecan treated for longer time points of 40 and 60 min (Fig. 6*A*). Robust endocytosis of HA was observed with RCS cells incubated with HA alone (Fig. 6*B*). The level of internalization was substantially reduced when cells were incubated with HA + intact PG (Fig. 6*C*). With only 10 min of clostripain treatment of the aggrecan monomer, the HA + PG aggregate resulted in more RCS cells with green fluorescence-positive vesicles (Fig. 6*D*), a significant increase over the HA + intact PG conditions observed in Fig. 6*H*. Cells incubated with HA + PG aggregates with 40 or 60 min of clostripain exposure exhibited substantially higher FITC-HA endocytosis levels (Fig. 6, *F* and *G*), with some of the high-end outlier cells (Fig. 6*H*, *closed circles*) within the same mean pixel intensity range as cells incubated with FITC-HA alone. These results suggest limited C-terminal cleavage of PG monomers proportionately removes the aggrecan-mediated impediment to HA internalization.

Additional experiments were performed to narrow the time range in which clostripain cleavage of aggrecan affects HA endocytosis. Fig. 6*I* depicts RCS cells incubated with HA alone, and Fig. 6*J* depicts cells incubated with HA + intact PG. In this series, 5 and 10 min of clostripain exposure (Fig. 6, *K* and *L*) resulted in a small but nonetheless significant increase in FITC-HA + PG endocytosis (quantified in Fig. 6*Q*). However, 15 min of clostripain exposure (Fig. 6*N*) resulted in a larger jump in FITC-HA + PG endocytosis, nearly equivalent to HA alone (Fig. 6*Q*). Robust HA + PG endocytosis was also observed using aggrecan exposed for 20 and 30 min to clostripain (Fig. 6, *O* and *P*). When mean pixel intensity from independent experiments was summarized (normalized to equivalent FITC-HA alone conditions (Fig. 6*R*)) the cutoff in aggrecan impedance of HA endocytosis occurred between 10 and 15 min of clostripain treatment. Nonetheless, even 5 and 10 min of clostripain cleavage allowed for significantly increased HA endocytosis as compared with intact aggrecan (Fig. 6*R*). Reducing the clostripain digestion time to between 0 and 10 min (Fig. 6*S*) in another set of two independent experiments confirmed that even limited aggrecan cleavage (Fig. 6*S*, *inset*) had an impact on promoting HA endocytosis. Although the clostripain time points of 0 to 10 min are clearly significantly reduced as compared with HA alone (Fig. 6*S*, *asterisks*), the 2–10-min time points were each significantly higher in mean pixel intensity than HA + intact PG. This suggests that only minor processing of aggrecan can begin to release the HA endocytosis block.

Effect of HA Size on HA Endocytosis—Another means of reducing the size of HA + PG aggregates is to alter the size of the HA molecule. Time-dependent sonication at 4 °C was used to selectively reduce the HA size of a particular FITC-HA preparation without changing the concentration or fluorescein conjugation-specific activity. Sonication for 5–30 s generated a roughly proportional series of HA species of reduced length (Fig. 7*I*). Using the endocytosis of intact FITC-HA as the posi-

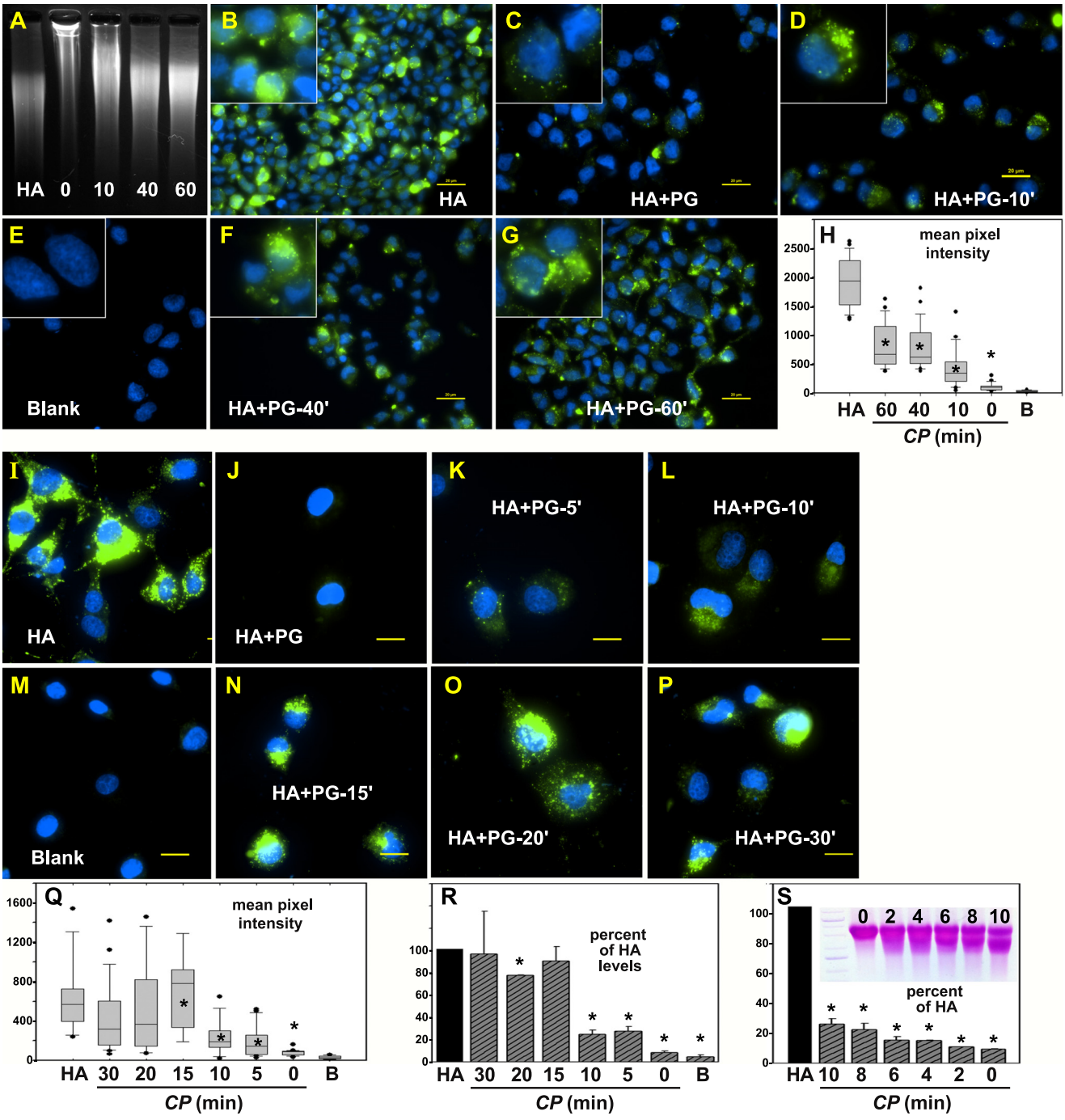

FIGURE 6. **Effect of limited C-terminal cleavage of aggrecan on HA endocytosis.** *A*, depicts UV transilluminator imaging of FITC-HA alone (*HA*) or FITC-HA combined with 0-, 10-, 40-, and 60-min clostripain-digested aggrecan monomers following agarose gel electrophoresis. Each fraction was then added individually (*B–G*) to hyaluronidase-pretreated RCS cells for 24 h at 37 °C followed by post-treatment with *Streptomyces* hyaluronidase. Thus all images depict intracellularly localized FITC-HA. All *bars* are 20 μm. High power images of individual cells are shown as *insets*. The mean pixel intensity of 25–30 cells/each experimental condition (HA alone or HA + aggrecan treated with CP for 0–60 min (*HA + PG*)) was evaluated (*H*). Shown are the box plots of mean pixel intensities from RCS cells that accumulated intracellular FITC-HA following the addition of HA alone or various HA + PG preparations including control untreated cells (*B*, indicates blank). The mean pixel intensities of cells recorded as outliers are included and shown as *round dots* (●). Student's *t* test comparisons were performed under the HA alone condition and under each of the HA + PG conditions. *Asterisks*, denote $p < 0.05$. The next set of experiments tested endocytosis of HA + aggrecan with clostripain treatment for 0 to 30 min. RCS cells were incubated with HA alone (*I*), with HA+ intact PG (*J*), and then with HA + clostripain-treated PG: 5-min treatment (*K*), 10-min treatment (*L*), 15-min treatment (*N*), 20-min treatment (*O*), and 30-min treatment (*P*). All *bars* are 20 μm. Mean pixel intensity of 25–30 cells/each experimental condition (HA alone or HA + aggrecan treated with CP for 0–30 min (*HA+PG*)) was evaluated (*Q*). Shown are the box plots of the mean pixel intensities in RCS cells that accumulated intracellular FITC-HA following the addition of HA alone or of various HA + PG preparations including control untreated cells (*Blank* in *M*). *B*, indicates blank (in *H*, *Q*, and *R*). The *bar graph* in *R* represents the mean pixel intensity average ± S.D. of two independent experiments and illustrates the normalized percent change in mean pixel intensity of HA + clostripain-treated PG (for 0–30 min) as compared with RCS cells treated with HA alone (set to 100%). *Asterisks*, denote $p < 0.05$. *S*, represents the mean pixel intensity average ± S.D. of two independent experiments and illustrates the normalized percent change in mean pixel intensity of HA + clostripain-treated PG (for only 0–10 min) as compared with RCS cells treated with HA alone (set to 100%). The *inset* in *S* depicts the migration of aggrecan after digestion for 0–10 min with CP.

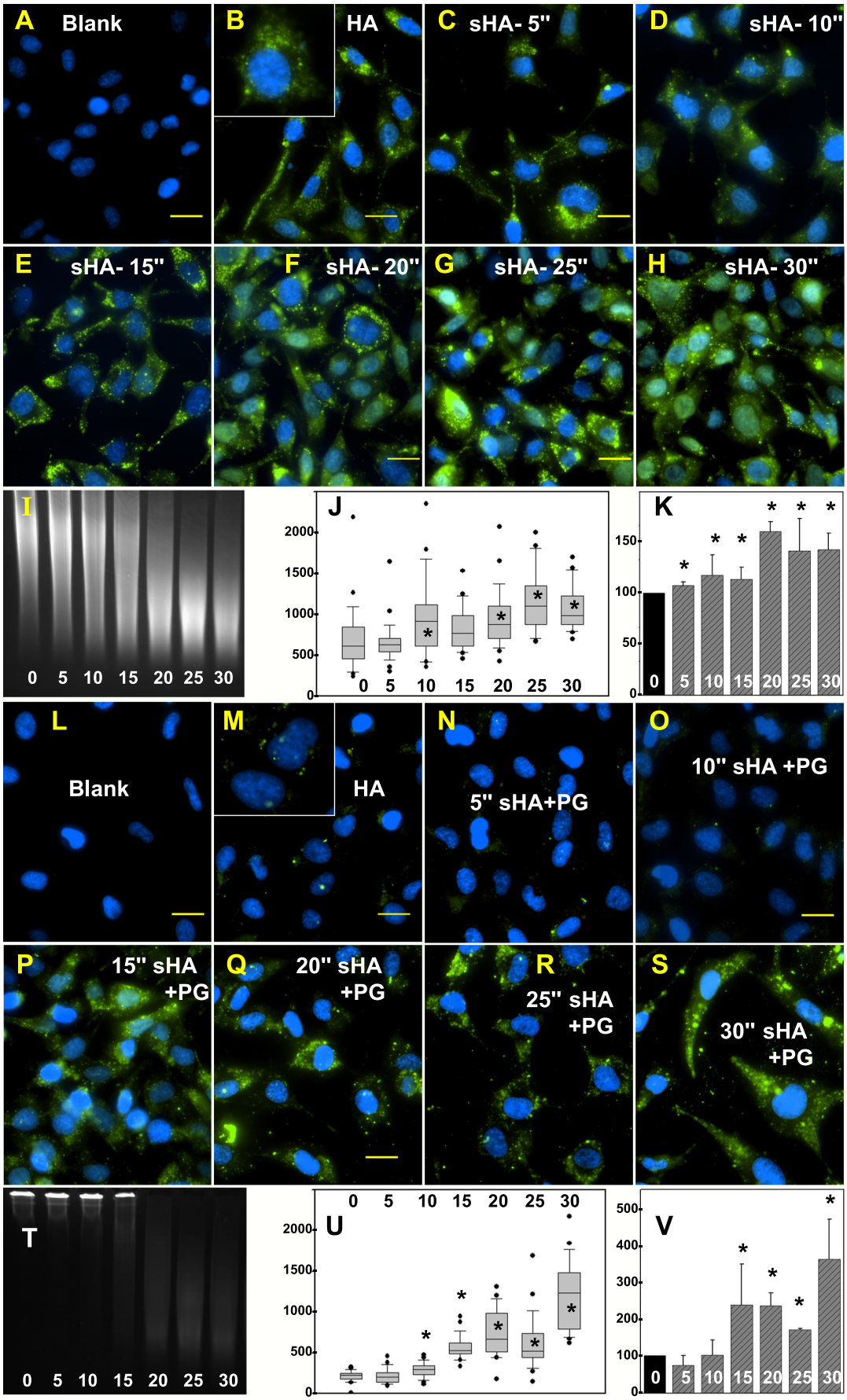
A Blank
B HA
C sHA- 5"
D sHA- 10"
E sHA- 15"
F sHA- 20"
G sHA- 25"
H sHA- 30"
I
0 5 10 15 20 25 30
J
2000
1500
1000
500
0
0 5 10 15 20 25 30
K
150
100
50
0
0 5 10 15 20 25 30
L Blank
M HA
N 5" sHA+PG
O 10" sHA +PG
P 15" sHA +PG
Q 20" sHA +PG
R 25" sHA +PG
S 30" sHA +PG
T
0 5 10 15 20 25 30
U
0 5 10 15 20 25 30
2000
1500
1000
500
V
500
400
300
200
100
0
0 5 10 15 20 25 30

tive control (Fig. 7*B*), a 5-s sonication of the FITC-HA preparation resulted in little comparative change in HA endocytosis (Fig. 7*C* and quantified in Fig. 7, *J* and *K*). However, after 10 s of sonication, a clearly discernable increase in HA endocytosis was observed (Fig. 7*D*), with incremental increases proportional to the sonication time until reaching a maximum at 25 s. Several cells incubated with sonicated HA accumulated intense intracellular deposits of ligand such that these cells were designated as high outliers and were not included in the calculation of mean pixel intensities (Fig. 7*J*). An analysis of four independent experiments is shown in Fig. 7*K* as percent of positive control (HA with no sonication).

In a second series of experiments, preparations of FITC-HA sonicated for 0–30 s were combined with intact aggrecan monomer. The combination with aggrecan size shifted the intact FITC-HA as well as FITC-HA sonicated for 5, 10, and 15 s into the loading wells of agarose gels (Fig. 7*T*); no shifting was observed with longer sonication time preparations. When intact HA + intact PG was incubated with RCS cells, little internalization of HA was observed (Fig. 7*M*). Little increase in internalized HA was observed in 5- or 10-s sonicated HA + intact aggrecan (Fig. 7, *N* and *O*). However, with sonication times of 15 s or longer, a clear and progressive increase in FITC-HA + intact aggrecan endocytosis was observed (Fig. 7, *P*–*S*). A box plot illustrates this significant change that occurred at 15 s of sonication (Fig. 7*U*), an event that was observed consistently upon repetition (Fig. 7*V*). It is possible that the 20-, 25-, and 30-s sonicated FITC-HA fractions were too short in HA length to retain an aggrecan monomer, consistent with the lack of size-shifting migration, as shown in Fig. 7*T*. However, both the 10- and 15-s sonicated HA + PG mixtures formed aggregates (Fig. 7*T*). The abrupt change in HA endocytosis between these two fractions (Fig. 7, *O* and *P*) suggests that only a limited number of proteoglycans bound to HA is necessary to impede HA endocytosis. However, it is unclear whether the increase in HA endocytosis observed in the 15-s sonicated HA + intact PG experiment (Fig. 7*P*) represents internalization of non-decorated FITC-HA or the co-internalization of an intact aggrecan.

Effect of C-terminal Cleavage of Aggrecan on Aggrecan Endocytosis—The data shown in Fig. 6 demonstrate that after extended clostripain cleavage of aggrecan, HA + PG endocytosis is increased to levels only slightly less than endocytosis of HA alone. However, these results are dependent on following the labeled HA. To determine whether the clostripain-cleaved aggrecan in the HA + PG aggregate was co-internalized, the aggrecan core protein was labeled with dansyl chloride as the fluorescent marker. As shown in Fig. 8*B*, the addition of HA + intact dansyl-PG aggregates to RCS cells resulted in no endocytosis of the PG. However, when cells were incubated with HA + dansyl-PG treated with clostripain for 30 min (conditions that mimic the experiment shown in Fig. 6*P*), intracellular blue fluorescent vesicles were readily apparent. The results from two independent experiments are shown in Fig. 8, *D* and *E*. Thus the increase in HA endocytosis observed in Fig. 6*P* was not due to the internalization of residual-free HA not decorated with aggrecan. Even after 30 min of clostripain cleavage (Fig. 8*F*), the smaller aggrecan monomer remained bound to HA and was co-internalized. Similarly, when intact dansyl-PG was allowed to re-aggregate with 15 -s sonicated HA and added to RCS cells, a dim but detectable intracellular blue fluorescence was observed (Fig. 8*C*). A modest shift in migration was observed for dansyl-PG-treated with clostripain for 30 min (Fig. 8*F*). To verify that dansyl-PG retained a functional capacity to bind to HA, it was mixed with HA or HA sonicated for 15 s; reaggregation was detected as a size shift to the loading wells of the agarose gel with blue fluorescence detected under UV transillumination (Fig. 8*G*, *lanes 1* and *2*). Dansyl-PG pretreated with clostripain and then combined with HA also exhibited a size shift to the loading well of the agarose gel (Fig. 8*G*, *lane 3*). Upon quantification, a statistically significant higher level of cell-localized blue fluorescence pixel intensity, above that of the blank control or full-length FITC-HA + intact PG, was observed (Fig. 8, *H* and *I*). Fig. 8, *H* and *I*, also demonstrates that the endocytosis of intact aggrecan bound to 15-s sonicated HA (*box* and *bar*, respectively, labeled *s0*) is statistically significant. We propose that this shortened length of sonicated HA contains fewer aggrecan monomers, perhaps as few as one intact proteoglycan per HA chain. As such, the level of overall fluorescence intensity would be greatly reduced. However, we cannot rule out that this limited HA-bound aggrecan could also have been proteolytically processed by endogenous endoproteinases during the incubation period.

DISCUSSION

Chondrocytes and many cell types exhibit large, HA-dependent pericellular matrices (17, 18). When these matrices are removed, the addition of exogenous HA together with aggrecan can rapidly re-establish these coats even on non-living, fixed cells (17, 18, 51). All that is required is an HA receptor such as CD44, HA, or aggrecan. We have also shown that CD44 mediates the endocytosis of HA as well as the co-internalization of bound aggrecan G1 domains including G1-ITEGE and G1-DIPEN (4, 7–9). It has been of interest to determine how cells such as chondrocytes regulate seemingly opposite func-

FIGURE 7. **Effect of HA size on HA endocytosis.** Endocytosis of FITC-HA by RCS cells (*B*) was compared with endocytosis of FITC-HA following sonication for 5 s (*C*), 10 s (*D*), 15 s (*E*), 20 s (*F*), 25 s (*G*), and 30 s (*H*). *A* and *L*, depict RCS cells with no addition. All *bars* are 20 μm. *I*, depicts UV transilluminator-dependent imaging of FITC-HA by agarose gel electrophoresis following sonication for 0–30 s. The mean pixel intensity of 25–30 cells/each experimental condition (FITC-HA sonicated for 0 to 30 s) was evaluated (*J*). Shown are the box plots of mean pixel intensities in RCS cells that accumulated intracellular FITC-HA. The *bar graph* in *K* represents the mean pixel intensity average ± S.D. of four independent experiments and illustrates the normalized percent change in mean pixel intensity of FITC-HA + sonication (for 5–30 s) as compared with RCS cells incubated with non-sonicated FITC-HA (set to 100%). *Asterisks*, denote $p < 0.05$. Intact aggrecan monomer was combined with FITC-HA that had been sonicated for varying times, added to RCS cells, and processed to visualize FITC-HA internalization. Sonication times were 0 s (*M*), 5 s (*N*), 10 s (*O*), 15 s (*P*), 20 s (*Q*), 25 s (*R*), and 30 s (*S*). All *bars* are 20 μm. The combination of intact aggrecan with intact FITC-HA (0 s) as well as with FITC-HA sonicated for 5–30 s was observed under UV transillumination following agarose gel electrophoresis (*T*). The mean pixel intensity of 25–30 cells/each experimental condition (FITC-HA sonicated for 0–30 s) was evaluated (*U*). Shown are the box plots of mean pixel intensities in RCS cells that accumulated intracellular FITC-HA. The *bar graph* in *V* represents the mean pixel intensity average ± S.D. of four independent experiments and illustrates the normalized percent change in mean pixel intensity of FITC-HA + sonication (for 5–30 s) as compared with RCS cells incubated with FITC-HA alone (set to 100%). *Asterisks*, denote $p < 0.05$.

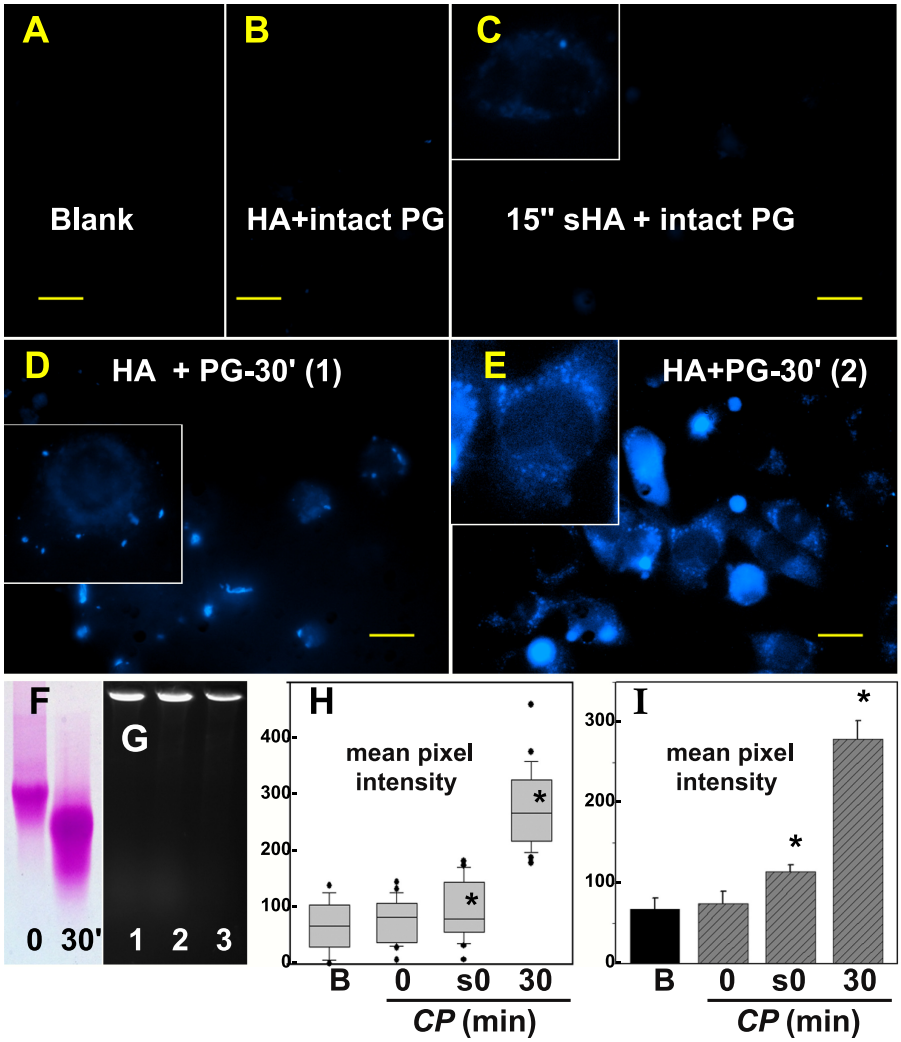

FIGURE 8. **Effect of C-terminal cleavage of aggrecan on HA/aggrecan endocytosis.** Aggrecan core protein was labeled with dansyl chloride as a blue fluorescent marker. *A*, shows low autofluorescence of RCS cells in the blue channel (*Blank*). RCS cells were then incubated with HA + intact dansyl-PG (*B*) or with HA + dansyl-PG treated with clostripain for 30 min (*D* and *E*). Similarly, intact dansyl-PG following re-aggregation with 15-s sonicated HA was added to RCS cells (*C*). All *bars* are 20 μm. High power images of individual cells are shown as *insets* (*C–E*). Size differences between intact dansyl-PG (0 s) and dansyl-PG treated with clostripain for 30 min (*30′*) were detected on 1% agarose gels stained with DMMB (*F*). Dansyl-PG mixed with HA (*G*, *lane 1*) or HA sonicated for 15 s (*G*, *lane 2*) exhibited a size shift to the loading wells of the agarose gel. Blue fluorescence was detected by UV transillumination. Dansyl-PG pretreated with clostripain for 30 min and then combined with HA also exhibited a size shift (*G*, *lane 3*). *H* and *I*, the mean pixel intensity of 25–30 cells/each experimental condition (*B*, blank; *0*, HA + intact dansyl-PG; *s0*, 15-s sonicated HA + intact dansyl-PG; *30*, HA + dansyl-PG treated with CP for 30 min was evaluated as a box plot (*H*). Shown are the box plots of mean pixel intensities in the blue channel (dansyl chloride) that accumulated in RCS cells. The *bar graph* in *I* represents the mean pixel intensity average ± S.D. of three independent experiments. *Asterisks* denote *p* value < 0.05.

tions of CD44 and HA, namely, HA-rich pericellular matrix retention and HA-matrix turnover. These cell surface events extend out to the tissue wherein proteoglycans such as aggrecan are enzymatically processed within the extracellular matrix with end products diffusing out of the tissue. HA, on the other hand, has mechanisms available for local turnover by receptor-mediated endocytosis. Some investigators have suggested that HA diffusion from cartilage can be substantial (52, 53), whereas others have estimated that diffusion accounts for 9% of the total HA lost from cartilage (15). It remains necessary to determine a mechanism to explain why the turnover half-life of newly synthesized HA and aggrecan in cartilage explants is nearly identical (15, 33). The results of this study address this mechanism.

One clear observation of this study is that the binding of intact aggrecan monomer to HA results in a nearly complete blockage of HA endocytosis. This suggests that little local turnover of HA occurs *in vivo* until some degree of aggrecan processing has occurred. The second important observation was that a reduction in the size of the aggrecan monomer, by seemingly modest size changes, removes the proteoglycan impediment to HA endocytosis. The HA itself may become degraded within the extracellular environment by hyaluronidases or free radicals (14). Nonetheless, if the shortened HA length is sufficient to bind a particular number of aggrecan monomers (as in Fig. 7, *N* and *O*), HA internalization will continue to be blocked. Thus, it is the release from the aggrecan block that is the likely mechanism responsible for nearly equivalent turnover half-lives of aggrecan and HA (15, 33). Moreover, such a mechanism would facilitate either mode of HA turnover, local endocytosis or diffusion out of the tissue. We do not know whether the same inhibition of HA endocytosis occurs with other aggregating proteoglycans such as versican (54–58), neurocan, and brevi-

can (59–61) but predict that their inhibitory potential would be dependent on the size, charge, or cross-linking domains uniquely associated with these proteoglycans.

The overall size and/or charge of large macromolecules such as aggrecan is the likely mechanism responsible for the blockage of HA endocytosis. Each aggrecan monomer bound to HA has a molecular mass of $>10^6$ daltons (62). With limited C-terminal cleavage of aggrecan, a break point in the blocking capacity appears between 10 and 15 min of clostripain digestion of aggrecan (Figs. 6*D* and 7, *L*, *N*, and *R*). A significant jump in HA endocytosis was observed when FITC-HA was decorated with the 15-min digested monomer. In fact, the endocytosis associated with this condition was not significantly different from FITC-HA with no aggrecan bound (Figs. 6*B* and 7*B*). The 15-min digested aggrecan does appear slightly more degraded than the monomer treated for 10 min (Fig. 5*A*), but the change in migration on agarose gels, from 0 to 30 min of digestion, is gradual (Fig. 5*A*), exhibiting no major jump in size between 10 and 15 min. Moreover, all aggrecan fractions between 0 and 30 min readily formed reconstituted aggregates with HA (Fig. 5*B*). Thus, although we do not (and likely never will) know the exact cutoff size of aggrecan that inhibits or permits HA endocytosis, it is clear that such a size exists.

With time points shorter than 10 min of clostripain exposure, HA endocytosis is observed, albeit at a substantially reduced level (Fig. 6, *K* and *Q*–*S*). Even as short a time as 2 min of exposure of aggrecan to clostripain provides for an increase in HA endocytosis that is statistically significant above that of intact aggrecan-containing aggregates (Fig. 6, *J versus K*). One possibility is that some important protein domain present on aggrecan is removed during the early time periods of clostripain digestion, such as the removal of the C-terminal G3 domain of the monomer. It has long been suggested that the G3 domain participates in cross-linking of aggrecan monomers (63), an activity that would allow pericellular coats to grow as wide as one cell diameter. For example, the G3 domain of aggrecan has been shown to cross-link with other aggrecan G3 domains via tenascin-C (63). It is not known whether the RCS cells synthesize sufficient tenascin-C, or some other cross-linking species, to promote such cross-links. However, we did observe that the addition of the purified aggrecan directly to RCS cells *in vitro* resulted in large, expanded pericellular matrices in as little as 1 h (Fig. 2*E*). Future studies will be needed to determine whether the aggrecan used in this study (purified from the cartilage of young cattle) retains the G3 domain and whether this G3 was lost by short-term clostripain digestion as in Fig. 6*S*. Nonetheless, the loss of an aggrecan cross-linking domain could provide an additional mechanism to relieve the HA endocytosis block. It should also be noted that during the aging process, cartilage aggrecan becomes reduced in size, including the proteolytic loss of G3 domains, shortening of the core protein, and shortening of chondroitin sulfate chains during biosynthesis (64, 65). We predict that HA turnover would be more prominent with age.

Another method of investigating the restrictions of HA endocytosis based on size was to generate HA chains shortened by sonication. FITC-HA endocytosis was enhanced proportional to the length of the sonication time (Fig. 7, *C*–*H*). It has long been known that shorter HA chains are internalized more efficiently than high molecular mass HA (66), but it is also clear that intact HA ($>10^6$ Da) is internalized directly without extracellular processing (4). Nonetheless, the point of these experiments was to demonstrate that size matters, including the size of the HA itself with no aggrecan bound. There are no precise data for the shortened sizes of the sonicated HA other than those noted by changes in migration on 1% agarose gels. However, the profile of these sonicated preparations, as shown in Fig. 7*I*, indicates sizes within the range of the middle molecular mass HA (shown in Fig. 1, *A* and *B*). Again, the precise size is not as critical as the functional size. The addition of intact aggrecan monomer to sonicated HA resulted in the formation of HA + PG aggregates except when HA was sonicated longer than 20 s (Fig. 7*T*). One interpretation is that the HA sonicated longer than 20 s was too short to allow aggrecan binding. Nonetheless, the goal of this approach was to observe the effects of aggrecan on a HA species that was sufficiently short such that it could only support the binding of a minimal number of intact aggrecans, perhaps even a single monomer. Our best model of such a species is the 15-s sonicated HA + PG aggregate. Although clearly a HA + PG aggregate (Fig. 7*T*), this complex permits HA endocytosis (Fig. 7*P*), whereas the 10-s sonicated HA + PG preparation (also an aggregate, Fig. 7*P*) blocked HA endocytosis (Fig. 7*O*). We propose that the 10-s sonicated HA + PG aggregate is long enough to retain multiple aggrecan monomers, whereas the 20-s sonicated HA is incapable of binding any aggrecan. Together the data suggest that there is an overall size limit for HA + PG aggregates that is restrictive for HA endocytosis. These results also demonstrated that it is possible that HA with one or a few bound intact aggrecan monomers (as in Fig. 7*P*) is not blocked from undergoing endocytosis. However, the latter conclusion would imply that the aggrecan itself is co-internalized with the HA. As an alternative explanation, sufficient FITC-HA not sequestered into an HA + PG aggregate could have contributed to the high level of internalized HA observed in Fig. 7*P*.

To address this question, aggrecan was fluorescently labeled with dansyl chloride (42, 43), a conjugation that did not interfere with HA binding (Fig. 8*G*). Following the addition of HA, combined with dansylated PG pretreated with clostripain for 30 min, to RCS cells *blue* fluorescent intracellular vesicles were observed (Fig. 8, *D* and *E*). We had observed previously the co-internalization of HA and aggrecan G1 domains (7–9); however these small globular domains carry little substitution with chondroitin sulfate or keratan sulfate as would be represented by the strongly DMMB-positive band shown in Fig. 8*F* or by the shift with HA into the loading well of an agarose gel (Fig. 5*B*). Thus, partially degraded aggrecan can be internalized by RCS cells. Given that no aggrecan receptor has ever been documented and that this preparation forms an HA + PG aggregate (Fig. 5*B*), we propose that the dansylated proteoglycan was co-internalized with HA. Faint, but discernable intracellular *blue* fluorescence was also observed when HA + PG aggregates were prepared with intact dansylated aggrecan mixed with 15-s sonicated HA (Fig. 8*C*). Although this may represent the internalization of a single or few intact aggrecan monomers, we are more cautious at this point. It remains a possibility that during

the 24-h incubation period, endogenous proteinases released into the culture medium sufficiently degraded the dansylated aggrecan so as to allow its endocytosis as observed in Fig. 8, *D* and *E*. Nonetheless, a straightforward conclusion is that it is overall size that matters with regard to endocytosis, regardless of glycosaminoglycan.

We have shown that CD44 itself undergoes co-internalization with HA endocytosis (67, 68). In fact, HA itself is an impediment to CD44 endocytosis. HA + PG-depleted bovine chondrocytes internalize/cycle 20% of their cell surface CD44 intracellularly within a 4-h period, whereas only 6% is internalized when the CD44 is occupied with HA (67). As such, one can speculate on another biological significance of aggrecan impendence of HA (and CD44) endocytosis. CD44 has been shown to interact and co-immunoprecipitate with several signaling receptors including EGF and TGFβ receptors (69–71). HA + PG aggregates bound to CD44 would limit the endocytosis/cycling of CD44 as well as any receptors tethered to CD44. Extracellular protease cleavage of aggrecan would release the HA endocytosis block, resulting in HA-CD44 endocytosis and permitting kinase receptor turnover.

In this study we have demonstrated the usefulness of visualizing highly polydisperse matrix macromolecules such as HA and aggrecan using agarose gel electrophoresis. This technique provides an effective way to observe the shift in size of HA and aggrecan when the two components are allowed to re-aggregate and to view the fragmentation of the two following sonication or enzymatic cleavage. Stains-all detected HA (*light blue*), proteoglycans (*dark blue* to *purple*), and the DNA standards (Fig. 1*C*). DMMB was more selective, marking the sulfated proteoglycans as *reddish blue-pink* bands depending on the amount of background destaining, whereas HA by itself was not stained (Figs. 1*D* and 2*A*). Interestingly, HA + PG aggregates were *purple* with DMMB staining (Figs. 2*B* and 5, *B* and *C*), although this could have been due to the clustering of proteoglycans on HA during the formation of aggregates. The 1000-bp incremented DNA standards were useful in normalizing aggrecan migration patterns from experiment to experiment. The intact aggrecan monomer typically migrated between the 3000- and 6000-bp standard bands.

Acknowledgments—We thank Michelle Cobb, Joani Zary Oswald, and Dr. Joseph Chalovich for technical assistance with this project.

REFERENCES

1. Fraser, J. R., Kimpton, W. G., Laurent, T. C., Cahill, R. N., and Vakakis, N. (1988) Uptake and degradation of hyaluronan in lymphatic tissue. *Biochem. J.* **256,** 153–158
2. Harris, E. N., Weigel, J. A., and Weigel, P. H. (2008) The human hyaluronan receptor for endocytosis (HARE/Stabilin-2) is a systemic clearance receptor for heparin. *J. Biol. Chem.* **283,** 17341–17350
3. Prevo, R., Banerji, S., Ferguson, D. J., Clasper, S., and Jackson, D. G. (2001) Mouse LYVE-1 is an endocytic receptor for hyaluronan in lymphatic endothelium. *J. Biol. Chem.* **276,** 19420–19430
4. Hua, Q., Knudson, C. B., and Knudson, W. (1993) Internalization of hyaluronan by chondrocytes occurs via receptor-mediated endocytosis. *J. Cell Sci.* **106,** 365–375
5. Jiang, H., Knudson, C. B., and Knudson, W. (2001) Antisense inhibition of alternatively spliced CD44 variant in human articular chondrocytes promotes hyaluronan internalization. *Arthritis Rheum.* **44,** 2599–2610
6. Jiang, H., Peterson, R. S., Wang, W., Bartnik, E., Knudson, C. B., and Knudson, W. (2002) A requirement for the CD44 cytoplasmic domain for hyaluronan binding, pericellular matrix assembly, and receptor-mediated endocytosis in COS-7 cells. *J. Biol. Chem.* **277,** 10531–10538
7. Embry, J. J., and Knudson, W. (2003) G1 domain of aggrecan cointernalizes with hyaluronan via a CD44-mediated mechanism in bovine articular chondrocytes. *Arthritis Rheum.* **48,** 3431–3441
8. Embry Flory, J. J., Fosang, A. J., and Knudson, W. (2006) The accumulation of intracellular ITEGE and DIPEN neoepitopes in bovine articular chondrocytes is mediated by CD44 internalization of hyaluronan. *Arthritis Rheum.* **54,** 443–454
9. Ariyoshi, W., Knudson, C. B., Luo, N., Fosang, A. J., and Knudson, W. (2010) Internalization of aggrecan G1 domain neoepitope ITEGE in chondrocytes requires CD44. *J. Biol. Chem.* **285,** 36216–36224
10. Culty, M., Nguyen, H. A., and Underhill, C. B. (1992) The hyaluronan receptor (CD44) participates in the uptake and degradation of hyaluronan. *J. Cell Biol.* **116,** 1055–1062
11. Culty, M., Shizari, M., Thompson, E. W., and Underhill, C. B. (1994) Binding and degradation of hyaluronan by human breast cancer cell lines expressing different isoforms of CD44: correlation with invasive potential. *J. Cell. Physiol.* **160,** 275–286
12. Tammi, R., Rilla, K., Pienimaki, J. P., MacCallum, D. K., Hogg, M., Luukkonen, M., Hascall, V. C., and Tammi, M. (2001) Hyaluronan enters keratinocytes by a novel endocytic route for catabolism. *J. Biol. Chem.* **276,** 35111–35122
13. Underhill, C. B., Nguyen, H. A., Shizari, M., and Culty, M. (1993) CD44 positive macrophages take up hyaluronan during lung development. *Dev. Biol.* **155,** 324–336
14. Knudson, W., Chow, G., and Knudson, C. B. (2002) CD44-mediated uptake and degradation of hyaluronan. *Matrix Biol.* **21,** 15–23
15. Ng, C. K., Handley, C. J., Preston, B. N., and Robinson, H. C. (1992) The extracellular processing and catabolism of hyaluronan in cultured adult articular cartilage explants. *Arch. Biochem. Biophys.* **298,** 70–79
16. Hardingham, T. E., and Fosang, A. J. (1992) Proteoglycans: many forms and many functions. *FASEB J.* **6,** 861–870
17. Knudson, C. B. (1993) Hyaluronan receptor-directed assembly of chondrocyte pericellular matrix. *J. Cell Biol.* **120,** 825–834
18. Knudson, W., Aguiar, D. J., Hua, Q., and Knudson, C. B. (1996) CD44-anchored hyaluronan-rich pericellular matrices: an ultrastructural and biochemical analysis. *Exp. Cell Res.* **228,** 216–228
19. Sandy, J. D., and Verscharen, C. (2001) Analysis of aggrecan in human knee cartilage and synovial fluid indicates that aggrecanase (ADAMTS) activity is responsible for the catabolic turnover and loss of whole aggrecan, whereas other protease activity is required for C-terminal processing *in vivo*. *Biochem. J.* **358,** 615–626
20. Fosang, A. J., Rogerson, F. M., East, C. J., and Stanton, H. (2008) ADAMTS-5: the story so far. *Eur. Cell. Mater.* **15,** 11–26
21. Lark, M. W., Bayne, E. K., Flanagan, J., Harper, C. F., Hoerrner, L. A., Hutchinson, N. I., Singer, I. I., Donatelli, S. A., Weidner, J. R., Williams, H. R., Mumford, R. A., and Lohmander, L. S. (1997) Aggrecan degradation in human cartilage. *J. Clin. Invest.* **100,** 93–106
22. Tortorella, M. D., Burn, T. C., Pratta, M. A., Abbaszade, I., Hollis, J. M., Liu, R., Rosenfeld, S. A., Copeland, R. A., Decicco, C. P., Wynn, R., Rockwell, A., Yang, F., Duke, J. L., Solomon, K., George, H., Bruckner, R., Nagase, H., Itoh, Y., Ellis, D. M., Ross, H., Wiswall, B. H., Murphy, K., Hillman, M. C., Jr., Hollis, G. F., Newton, R. C., Magolda, R. L., Trzaskos, J. M., and Arner, E. C. (1999) Purification and cloning of aggrecanase-1: a member of the ADAMTS family of proteins. *Science* **284,** 1664–1666
23. Tortorella, M. D., Malfait, A. M., Deccico, C., and Arner, E. (2001) The role of ADAM-TS4 (aggrecanase-1) and ADAM-TS5 (aggrecanase-2) in a model of cartilage degradation. *Osteoarthr. Cartil.* **9,** 539–552
24. Stanton, H., Rogerson, F. M., East, C. J., Golub, S. B., Lawlor, K. E., Meeker, C. T., Little, C. B., Last, K., Farmer, P. J., Campbell, I. K., Fourie, A. M., and Fosang, A. J. (2005) ADAMTS5 is the major aggrecanase in mouse cartilage *in vivo* and *in vitro*. *Nature* **434,** 648–652
25. Abbaszade, I., Liu, R. Q., Yang, F., Rosenfeld, S. A., Ross, O. H., Link, J. R., Ellis, D. M., Tortorella, M. D., Pratta, M. A., Hollis, J. M., Wynn, R., Duke,

J. L., George, H. J., Hillman, M. C., Jr., Murphy, K., Wiswall, B. H., Copeland, R. A., Decicco, C. P., Bruckner, R., Nagase, H., Itoh, Y., Newton, R. C., Magolda, R. L., Trzaskos, J. M., and Burn, T. C. (1999) Cloning and characterization of ADAMTS11, an aggrecanase from the ADAMTS family. *J. Biol. Chem.* **274,** 23443–23450

26. Glasson, S. S., Askew, R., Sheppard, B., Carito, B., Blanchet, T., Ma, H. L., Flannery, C. R., Peluso, D., Kanki, K., Yang, Z., Majumdar, M. K., and Morris, E. A. (2005) Deletion of active ADAMTS5 prevents cartilage degradation in a murine model of osteoarthritis. *Nature* **434,** 644–648
27. Flannery, C. R., Lark, M. W., and Sandy, J. D. (1992) Identification of a stromelysin cleavage site within the interglobular domain of human aggrecan: evidence for proteolysis at this site in vivo in human articular cartilage. *J. Biol. Chem.* **267,** 1008–1014
28. Lohmander, L. S., Hoerrner, L. A., and Lark, M. W. (1993) Metalloproteinases, tissue inhibitor, and proteoglycan fragments in knee synovial fluid in human osteoarthritis. *Arthritis Rheum.* **36,** 181–189
29. Holmes, M. W., Bayliss, M. T., and Muir, H. (1988) Hyaluronic acid in human articular cartilage. *Biochem. J.* **250,** 435–441
30. Pita, J. C., Muller, F. J., Manicourt, D. H., Buckwalter, J. A., and Ratcliffe, A. (1992) Early matrix changes in experimental osteoarthritis and joint disuse atrophy, in *Articular Cartilage and Osteoarthritis* (Kuettner, K. E., Schleyerbach, R., Peyron, J. G., and Hascall, V. C., eds) pp 455–470, Raven Press, New York
31. Haapala, J., Lammi, M. J., Inkinen, R., Parkkinen, J. J., Agren, U. M., Arokoski, J., Kiviranta, I., Helminen, H. J., and Tammi, M. I. (1996) Coordinated regulation of hyaluronan and aggrecan content in the articular cartilage of immobilized and exercised dogs. *J. Rheumatol.* **23,** 1586–1593
32. Nishida, Y., D'Souza, A. L., Thonar, E. J., and Knudson, W. (2000) IL-1a stimulates hyaluronan metabolism in human articular cartilage. *Arthritis Rheum.* **43,** 1315–1326
33. Morales, T. I., and Hascall, V. C. (1988) Correlated metabolism of proteoglycans and hyaluronic acid in bovine cartilage organ cultures. *J. Biol. Chem.* **263,** 3632–3638
34. Mellor, L., Knudson, C. B., Hida, D., Askew, E. B., and Knudson, W. (2013) Intracellular domain fragment of CD44 alters CD44 function in chondrocytes. *J. Biol. Chem.* **288,** 25838–25850
35. Choi, H. U., Meyer, K., and Swarm, R. (1971) Mucopolysaccharide and protein-polysaccharide of a transplantable rat chondrosarcoma. *Proc. Natl. Acad. Sci. U.S.A.* **68,** 877–879
36. Kucharska, A. M., Kuettner, K. E., and Kimura, J. H. (1990) Biochemical characterization of long-term culture of the Swarm rat chondrosarcoma chondrocytes in agarose. *J. Orthop. Res.* **8,** 781–792
37. Knudson, W., Casey, B., Nishida, Y., Eger, W., Kuettner, K. E., and Knudson, C. B. (2000) Hyaluronan oligosaccharides perturb cartilage matrix homeostasis and induce chondrogenic chondrolysis. *Arthritis Rheum.* **43,** 1165–1174
38. Knudson, C. B., and Toole, B. P. (1985) Fluorescent morphological probe for hyaluronate. *J. Cell Biol.* **100,** 1753–1758
39. Hascall, V. C., Oegema, T. R., Brown, M., and Caplan, A. I. (1976) Isolation and characterization of proteoglycans from chick limb bud chondrocytes grown *in vitro*. *J. Biol. Chem.* **251,** 3511–3519
40. Caputo, C. B., MacCallum, D. K., Kimura, J. H., Schrode, J., and Hascall, V. C. (1980) Characterization of fragments produced by clostripain digestion of proteoglycans from the Swarm rat chondrosarcoma. *Arch. Biochem. Biophys.* **204,** 220–233
41. Guzik, K., Bzowska, M., Smagur, J., Krupa, O., Sieprawska, M., Travis, J., and Potempa, J. (2007) A new insight into phagocytosis of apoptotic cells: proteolytic enzymes divert the recognition and clearance of polymorphonuclear leukocytes by macrophages. *Cell Death Differ.* **14,** 171–182
42. Tengblad, A. (1979) Affinity chromatography on immobilized hyaluronate and its application to the isolation of hyaluronate binding properties from cartilage. *Biochim Biophys. Act.* **578,** 281–289
43. Bartzatt, R. (2001) Dansylation of hydroxyl and carboxylic acid functional groups. *J. Biochem. Biophys. Methods* **47,** 189–195
44. Cowman, M. K., Chen, C. C., Pandya, M., Yuan, H., Ramkishun, D., LoBello, J., Bhilocha, S., Russell-Puleri, S., Skendaj, E., Mijovic, J., and Jing, W. (2011) Improved agarose gel electrophoresis method and molecular mass calculation for high molecular mass hyaluronan. *Anal. Biochem.* **417,** 50–56
45. Bhilocha, S., Amin, R., Pandya, M., Yuan, H., Tank, M., LoBello, J., Shytuhina, A., Wang, W., Wisniewski, H. G., de la Motte, C., and Cowman, M. K. (2011) Agarose and polyacrylamide gel electrophoresis methods for molecular mass analysis of 5- to 500-kDa hyaluronan. *Anal. Biochem.* **417,** 41–49
46. Lee, H. G., and Cowman, M. K. (1994) An agarose gel electrophoretic method for analysis of hyaluronan molecular weight distribution. *Anal. Biochem.* **219,** 278–287
47. Wibo, M., and Poole, B. (1974) Protein degradation in cultured cells. II. The uptake of chloroquine by rat fibroblasts and the inhibition of cellular protein degradation and cathepsin B1. *J. Cell Biol.* **63,** 430–440
48. Dunmore, B. J., Drake, K. M., Upton, P. D., Toshner, M. R., Aldred, M. A., and Morrell, N. W. (2013) The lysosomal inhibitor, chloroquine, increases cell surface BMPR-II levels and restores BMP9 signalling in endothelial cells harbouring BMPR-II mutations. *Hum. Mol. Genet.* **22,** 3667–3679
49. Roughley, P. J., Melching, L. I., Heathfield, T. F., Pearce, R. H., and Mort, J. S. (2006) The structure and degradation of aggrecan in human intervertebral disc. *Eur. Spine J.* **15,** S326–S332
50. Lauer, M. E., Mukhopadhyay, D., Fulop, C., de la Motte, C. A., Majors, A. K., and Hascall, V. C. (2009) Primary murine airway smooth muscle cells exposed to poly(I,C) or tunicamycin synthesize a leukocyte-adhesive hyaluronan matrix. *J. Biol. Chem.* **284,** 5299–5312
51. Knudson, W., Bartnik, E., and Knudson, C. B. (1993) Assembly of pericellular matrices by COS-7 cells transfected with CD44 homing receptor genes. *Proc. Natl. Acad. Sci. U.S.A.* **90,** 4003–4007
52. Sztrolovics, R., Recklies, A. D., Roughley, P. J., and Mort, J. S. (2002) Hyaluronate degradation as an alternative mechanism for proteoglycan release from cartilage during interleukin-1B-stimulated catabolism. *Biochem. J.* **362,** 473–479
53. Durigova, M., Roughley, P. J., and Mort, J. S. (2008) Mechanism of proteoglycan aggregate degradation in cartilage stimulated with oncostatin M. *Osteoarthr. Cartil.* **16,** 98–104
54. Stupka, N., Kintakas, C., White, J. D., Fraser, F. W., Hanciu, M., Aramaki-Hattori, N., Martin, S., Coles, C., Collier, F., Ward, A. C., Apte, S. S., and McCulloch, D. R. (2013) Versican processing by a disintegrin-like and metalloproteinase domain with thrombospondin-1 repeats proteinases-5 and -15 facilitates myoblast fusion. *J. Biol. Chem.* **288,** 1907–1917
55. Hattori, N., Carrino, D. A., Lauer, M. E., Vasanji, A., Wylie, J. D., Nelson, C. M., and Apte, S. S. (2011) Pericellular versican regulates the fibroblast-myofibroblast transition: a role for ADAMTS5 protease-mediated proteolysis. *J. Biol. Chem.* **286,** 34298–34310
56. Evanko, S. P., Angello, J. C., and Wight, T. N. (1999) Formation of hyaluronan- and versican-rich pericellular matrix is required for proliferation and migration of vascular smooth muscle cells. *Arterioscler. Thromb. Vasc. Biol.* **19,** 1004–1013
57. Hudson, K. S., Andrews, K., Early, J., Mjaatvedt, C. H., and Capehart, A. A. (2010) Versican G1 domain and V3 isoform overexpression results in increased chondrogenesis in the developing chick limb *in ovo*. *Anat. Rec.* **293,** 1669–1678
58. Kern, C. B., Norris, R. A., Thompson, R. P., Argraves, W. S., Fairey, S. E., Reyes, L., Hoffman, S., Markwald, R. R., and Mjaatvedt, C. H. (2007) Versican proteolysis mediates myocardial regression during outflow tract development. *Dev. Dyn.* **236,** 671–683
59. Sherman, L. S., and Back, S. A. (2008) A "GAG" reflex prevents repair of the damaged CNS. *Trends Neurosci.* **31,** 44–52
60. Yamaguchi, Y. (2000) Lecticans: organizers of the brain extracellular matrix. *Cell. Mol. Life Sci.* **57,** 276–289
61. Ida, M., Shuo, T., Hirano, K., Tokita, Y., Nakanishi, K., Matsui, F., Aono, S., Fujita, H., Fujiwara, Y., Kaji, T., and Oohira, A. (2006) Identification and functions of chondroitin sulfate in the milieu of neural stem cells. *J. Biol. Chem.* **281,** 5982–5991
62. Buckwalter, J. A., and Rosenberg, L. C. (1982) Electron micrographic studies of cartilage proteoglycans. *J. Biol. Chem.* **257,** 9830–9839
63. Aspberg, A. (2012) The different roles of aggrecan interaction domains. *J. Histochem. Cytochem.* **60,** 987–996
64. Buckwalter, J. A., Kuettner, K. E., and Thonar, E. J. (1985) Age-related changes in articular cartilage proteoglycans: electron micrographic stud-

ies. *J. Orthop. Res.* **3,** 251–257
65. Sweet, M. B., Thonar, E. J., and Marsh, J. (1979) Age-related changes in proteoglycan structure. *Arch. Biochem. Biophys.* **198,** 439–448
66. McGuire, P. G., Castellot, J. J., Jr., and Orkin, R. W. (1987) Size-dependent hyaluronate degradation by cultured cells. *J. Cell. Physiol.* **133,** 267–276
67. Aguiar, D. J., Knudson, W., and Knudson, C. B. (1999) Internalization of the hyaluronan receptor CD44 by chondrocytes. *Exp. Cell Res.* **252,** 292–302
68. Thankamony, S. P., and Knudson, W. (2006) Acylation of CD44 and its association with lipid rafts are required for receptor and hyaluronan endocytosis. *J. Biol .Chem.* **281,** 34601–34609
69. Misra, S., Toole, B. P., and Ghatak, S. (2006) Hyaluronan constitutively regulates activation of multiple receptor tyrosine kinases in epithelial and carcinoma cells. *J. Biol. Chem.* **281,** 34936–34941
70. Ito, T., Williams, J. D., Fraser, D., and Phillips, A. O. (2004) Hyaluronan attenuates transforming growth factor-β1-mediated signaling in renal proximal tubular epithelial cells. *Am. J. Pathol.* **164,** 1979–1988
71. Takahashi, E., Nagano, O., Ishimoto, T., Yae, T., Suzuki, Y., Shinoda, T., Nakamura, S., Niwa, S., Ikeda, S., Koga, H., Tanihara, H., and Saya, H. (2010) Tumor necrosis factor-α regulates transforming growth factor-β-dependent epithelial-mesenchymal transition by promoting hyaluronan-CD44-moesin interaction. *J. Biol. Chem.* **285,** 4060–4073